ACS APPLIED MATERIALS & INTERFACES

Research Article

www.acsami.org

Formation Process of Eosin Y-Adsorbing ZnO Particles by Electroless Deposition and Their Photoelectric Conversion Properties

Satoshi Nagaya,[†] Hiromasa Nishikiori,*[,‡] Hideaki Mizusaki,[†] Hajime Wagata,[‡] and Katsuya Teshima[‡]

[†]Nagano Prefecture General Industrial Technology Center, 1-3-1, Osachi-Katamacho, Okaya, Nagano, 394-0084 Japan

[‡]Department of Environmental Science and Technology, Faculty of Engineering, Shinshu University, 4-17-1 Wakasato, Nagano, 380-8553 Japan

Supporting Information

ABSTRACT: The thin films consisting of crystalline ZnO particles were prepared on fluorine-doped tin oxide electrodes by electroless deposition. The particles were deposited from an aqueous solution containing zinc nitrate, dimethyamine−borane, and eosin Y at 328 K. As the Pd particles were adsorbed on the substrate, not only the eosin Y monomer but also the dimer and debrominated species were rapidly adsorbed on the spherical ZnO particles, which were aggregated and formed secondary particles. On the other hand, in the absence of the Pd particles, the monomer was adsorbed on the flake-shaped ZnO particles, which vertically grew on the substrate surface and had a high crystallinity. The photoelectric conversion efficiency was higher for the ZnO electrodes containing a higher amount of the monomer during light irradiation.

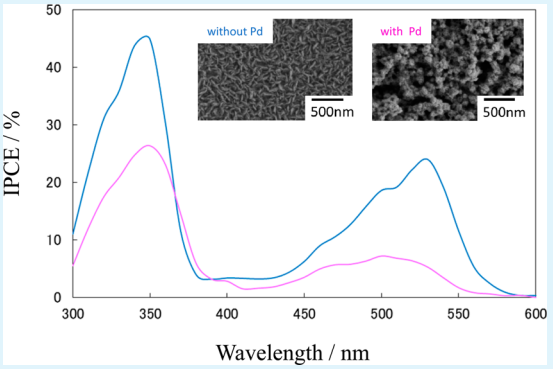

KEYWORDS: *palladium, ZnO, eosin Y, debromination, electroless deposition*

1. INTRODUCTION

Recently, the research and development of industrial products containing organic materials, such as functional polymers and dyes, have progressed. These are expected to be used as display and memory materials[1] and their demand will further increase in the electronics field. Among them, the interesting properties of organic dyes have been utilized in various studies. The dyes with colorful chromophores, such as diarylethenes[2,3] and spiropyrans,[4,5] have been used as photochromic materials based on their color change due to their structural changes by external light stimulation. In addition, some dyes are expected to be used as functional materials for electroluminescence,[6] laser devices,[7] etc., and some of them are already in use. The detailed properties of the dyes should be understood to effectively use such materials. The organic−inorganic composite materials also attract considerable attention because they are expected to exhibit novel properties different from the individual properties of the original organic and inorganic materials.[8] Actually, they are used in photocatalysts[9] and photoelectric conversion devices[10] based on their dye sensitization in many studies.

Metal oxide semiconductors, such as titania, CuO, and ZnO, are used as inorganic materials in composites because the hybridization between the organic dyes and them, having unique properties, can create new functions. Among them, ZnO is prepared by various methods, i.e., ZnO was directly deposited from a $Zn(NO_3)_2$ or $ZnCl_2$ aqueous solution by electrodeposition[11,12] and electroless deposition,[13] which was developed in the 1990s. Such methods can produce ZnO at a low temperature and a low price. Furthermore, the organic dye-adsorbing ZnO was spontaneously formed by mixing the dye in a solution during the 2000s. Yoshida et al. applied the dye-adsorbing ZnO films prepared by this method to dye-sensitized solar cells.[14−16] This method allowed us to produce large-sized devices at a low temperature and a low price and contribute to the advancement of the electronics industries.

We previously prepared dye-adsorbing ZnO thin films by electroless deposition.[17] Compared to electrodeposition, electroless deposition can easily prepare films consisting of nanosized particles that have a high specific surface area due to their slow deposition rate.[12] In the study, we prepared eosin Y-adsorbing ZnO hybrid thin films from an aqueous solution containing $Zn(NO_3)_2$, dimethylamine−borane (DMAB), and eosin Y by electroless deposition and evaluated them for use as solar cell electrodes.[17]

During the electroless deposition process, it is effective to impart the Pd particles as a catalyst on the substrate surface before the electroless deposition.[13,18] The formation process of ZnO can be expressed as follows:[13]

$$(CH_3)_2NHBH_3 + H_2O \rightarrow BO_2^- + (CH_3)_2NH + 7H^+ + 6e^- \quad (1)$$

Received: March 23, 2015
Accepted: May 15, 2015
Published: May 15, 2015

DOI: 10.1021/acsami.5b02570
ACS Appl. Mater. Interfaces 2015, 7, 11592−11598

$$NO_3^- + H_2O + 2e^- \rightarrow NO_2^- + 2OH^- \quad (2)$$

$$Zn^{2+} + 2OH^- \rightarrow Zn(OH)_2 \quad (3)$$

$$Zn(OH)_2 \rightarrow ZnO + H_2O \quad (4)$$

The reduction by DMAB (eq 1) actively occurred on the Pd particles and promoted the subsequent reactions for deposition of the ZnO particles (eqs 2−4). Dye species in the aqueous solution, such as the monomer and dimer, were adsorbed on the ZnO particles at the same time where the ZnO had deposited. The electron injection process significantly depends on the dye species and the interaction between the dye and ZnO. However, the adsorbed dye species are not well-known. It is important to clarify the mechanisms of the ZnO particle formation, its crystal growth, and dye adsorption on the ZnO because the structures of the ZnO particles and dye affect the spectroscopic and electrochemical properties in a photovoltaic electrode. Besides, it is interesting to study the change in the dye-molecular species with the deposition of the ZnO particles.

In this study, we investigated the surface structural characterization and dye molecular species of the eosin Y-adsorbing ZnO particles prepared by electroless deposition on the substrates under various conditions and evaluated their spectroscopic and photoelectric conversion properties.

2. EXPERIMENTAL SECTION

2.1. Materials and Sample Preparation. The fluorine-doped tin oxide (FTO) glass plates (9 Ω cm^{-2}, AGC Fabritech) or glass plates (Matsunami Glass S1225) were coated with ca. 30-nm-thick ZnO thin films as a buffer layer[19] and used as the substrates. The main ZnO films were deposited from aqueous solutions containing reagent-grade chemicals and distilled water. The buffer layer was prepared by dip-coating in 2-methoxyethanol containing 0.25 mol dm^{-3} zinc acetate and 0.0125 mol dm^{-3} 2-aminoethanol. After the dip coating, the substrates were heat-treated at 723 K for 30 min. The FTO surface resistance was 15 Ω cm^{-2} after the heating.

The substrates with ZnO thin films were rinsed in 2-propanol and distilled water along with ultrasonication for 1 min. They were pretreated to adsorb the Pd^{2+}, and then they were immersed in an aqueous colloid solution prepared from 0.10 mol dm^{-3} tin(IV) chloride. $SnO_2{\cdot}xH_2O$ was supported as an adsorbent on the substrate surface.[17,20] They were washed with distilled water and then successively immersed in a 5.0 mmol dm^{-3} silver nitrate ($AgNO_3$) aqueous solution ($AgNO_3$ treatment) and 0−1.2 mmol dm^{-3} palladium(II) chloride ($PdCl_2$) aqueous solution ($PdCl_2$ treatment) for 1 min each. Finally, the Pd^{2+} was adsorbed on the surface. The Pd catalyst particles were produced by the DMAB reductant during the electroless deposition process.

Electroless deposition of the eosin Y-adsorbing ZnO films were conducted using an aqueous solution containing 0.050 mol dm^{-3} $Zn(NO_3)_2$, 0.025 mol dm^{-3} DMAB, and 70 μmol dm^{-3} eosin Y. The solution was prepared under the conditions of ca. pH 6 and stored at 333 K with stirring. After the electroless deposition, the substrates were washed with distilled water and dried at 343 and 423 K each for 30 min.

2.2. Measurements. The UV−vis absorption spectra of the samples were measured using a spectrophotometer (Hitachi U-4000). The eosin Y species in the films were determined by high-performance liquid chromatography−mass spectrometry (HPLC-MS, Waters QT of MS). The surface morphology of the samples was observed using a scanning electron microscope, and elemental analysis was conducted by energy-dispersive X-ray spectroscopy (SEM-EDS, JEOL JSM-6010LA and Carl Zeiss Ultraplus). The thickness of the films was obtained using an X-ray fluorescence analyzer (XRF, Seiko Instruments SEA5150). The X-ray diffraction patterns were obtained using an X-ray diffractometer (XRD, Rigaku RINT2100). For examination of the photoelectrochemical properties, the electrolyte solution consisting of acetonitrile and ethylenecarbonate (v/v = 1/4) containing 0.50 mol dm^{-3} KI and 0.030 mol dm^{-3} I_2 was allowed to soak into the space (using about a 4-μm spacer) between the working and counter Pt electrodes. The samples were irradiated with monochromatic light obtained from a fluorescence spectrophotometer (Hitachi F2000) with a Xe short arc lamp (irradiation area 0.32 cm^2). During the light irradiation, the short circuit current was measured in the range from 300 to 600 nm by a digital multimeter (Agilent 34405A). The J−V curves of the samples were measured by a potentiostat (Hokuto Denko HA-151B) during the light irradiation using the Xe short arc lamp with an air mass filter (350−1050 nm, 100 mW cm^{-2}).

3. RESULTS AND DISCUSSION

3.1. Influence of Pd on the Eosin Y Species. As soon as the glass substrates adsorbing Pd^{2+} were immersed in a 0.025 mol dm^{-3} DMAB aqueous solution, their color changed from colorless to brown, indicating that the Pd^{2+} was reduced to Pd metal by DMAB. The energy-dispersive X-ray spectroscopy (EDS) measurement detected low amounts of Sn and Pd in the film prepared after the treatment with the 1.2 mmol dm^{-3} $PdCl_2$ solution. It was presumed that the film after the $PdCl_2$ treatment was covered with the $SnO_2{\cdot}xH_2O$[20] and Pd^{2+}. The $AgNO_3$ treatment was expected to eventually increase the amount of the Pd particles adsorbed on the substrate.

Figure 1 shows the absorption spectra of the eosin Y-adsorbing ZnO films prepared after the treatment with the different concentrations of $PdCl_2$ solutions compared to that of the 0.24 mmol dm^{-3} eosin Y aqueous solution. The aqueous solution exhibited an absorption band having a peak at 515 nm assigned to the monomer of the eosin Y dianion.[7] The films prepared after the treatment with 0 and 0.024 mmol dm^{-3} $PdCl_2$ solutions exhibited an absorption band having a peak at 525 nm and a shoulder at 490 nm. Furthermore, the relative intensity of the shoulder at 490 nm increased with an increase in the concentration of $PdCl_2$ for the treatment. When the 1.2 mmol dm^{-3} $PdCl_2$ solution is used, the absorption peak of the film was located at 490 nm. The absorption peak at 525 nm assigned to the eosin Y dianion was red-shifted compared to the peak wavelength of eosin Y in the solution. The absorption peak at 490 nm was assigned to the dimer based on a previous

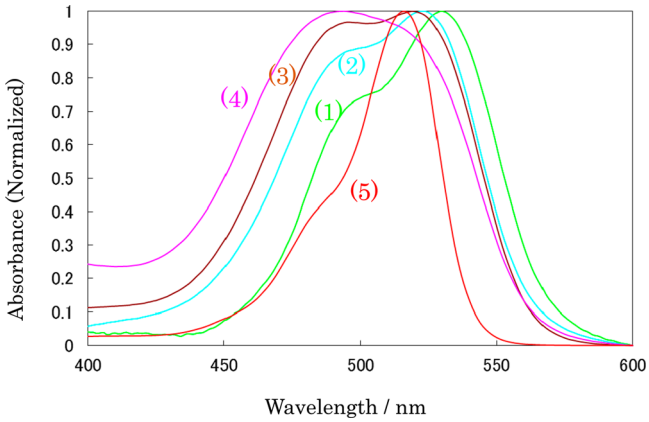

Figure 1. Absorption spectra of the eosin Y-adsorbing ZnO films prepared after the treatment with (1) 0, (2) 0.024, (3) 0.060, and (4) 1.2 mmol dm^{-3} $PdCl_2$ solutions compared to (5) that of the 0.24 mmol dm^{-3} eosin Y aqueous solution.

DOI: 10.1021/acsami.5b02570
ACS Appl. Mater. Interfaces 2015, 7, 11592−11598

paper.[7] We will discuss the assignment of this peak in detail based on the results of the HPLC-MS measurement.

Figure 2 shows the absorption spectra of the films prepared for the different deposition times after the treatment with 0 and 1.2 mmol dm^{-3} $PdCl_2$ solutions. During the initial stage of the electroless deposition, the film prepared on the substrate without Pd^{2+} exhibited an absorption peak at 525 nm due to the eosin Y dianion. However, the absorption peak intensity at 490 nm increased with the increasing deposition time. The film prepared on the substrate with Pd^{2+} exhibited an absorption peak at 490 nm even during the initial stage. The peak wavelength did not change with the increasing deposition time. The film thicknesses were determined to be 0.2, 1.5, 0.6, and 1.5 μm for the films prepared by 4-h deposition without Pd^{2+}, 14-h deposition without Pd^{2+}, 10-min deposition with Pd^{2+}, and 30-min deposition with Pd^{2+}, respectively. The thickness of the film prepared on the substrate with Pd^{2+} for only a 30-min deposition time was 1.5 μm, while in the case of no Pd^{2+}, it took more than 10 h to obtain the 1.5-μm-thick film. These results indicated that the amount of Pd particles on the surface increased the ZnO film thickness.

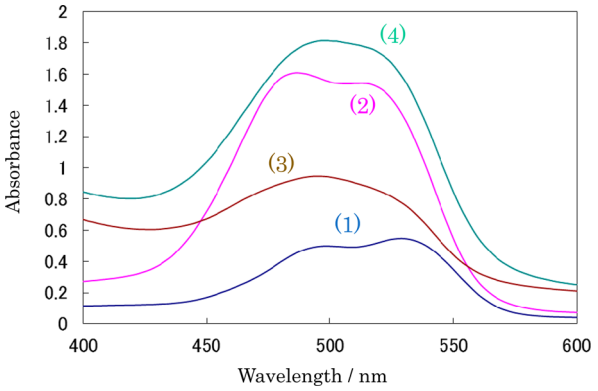

Figure 2. Absorption spectra of the eosin Y-adsorbing ZnO films prepared by (1) 4- and (2) 14-h depositions without Pd^{2+} and (3) 10- and (4) 30-min depositions after the treatment with 1.2 mmol dm^{-3} $PdCl_2$ solutions.

Eosin Y can be extracted from the ZnO film by immersing the film in a concentrated KOH aqueous solution.[21] Figure 3 shows the absorption spectra of films A and B and the KOH aqueous solutions which dissolved eosin Y from the films. Films A and B were prepared after the treatments with the 0.060 and 1.2 mmol dm^{-3} $PdCl_2$ solutions, respectively. The absorption peaks of these films were different, i.e., at 525 and 490 nm, respectively. The absorption spectra of the KOH solution prepared from film A had a maximum at 515 nm, which corresponds to the absorption peak of the eosin Y solution in Figure 1. The absorption spectra of the KOH solution prepared from film B has a peak at 500 nm and is broader compared to that of the eosin Y solution in Figure 1.

It was reported that the absorption peak of the eosin Y dimer was observed at 490 nm and the dimer dissociation constant in the aqueous solution at pH 12 was 9.0×10^{-3} mol dm^{-3}.[22] The absorption spectra of the films and solutions indicate that, in film A, the eosin Y formed not only the monomer but also the dimer, which was dissociated into the monomers in the KOH solution. If the eosin Y in film B forms the dimer, the absorption spectra of the KOH solution has a peak at 515 nm because the eosin Y dimer should be dissociated into the monomer similar to that of film A. However, in fact, the absorption peak of the KOH solution from film B was observed at 500 nm. It is suggested that other molecular species of the eosin Y, except for the dimer, existed in film B. To clarify the species of the eosin Y, the KOH solutions were analyzed by HPLC-MS.

Figure 4 shows the HPLC chromatograms of the KOH solutions. On the basis of the HPLC measurement of eosin Y in the KOH solutions, peak 3 at 15.8−15.9 min was assigned to the original eosin Y. The KOH solutions from the film showed other peaks at 8.8−9.0 min (peak 1) and at 12.4 min (peak 2).

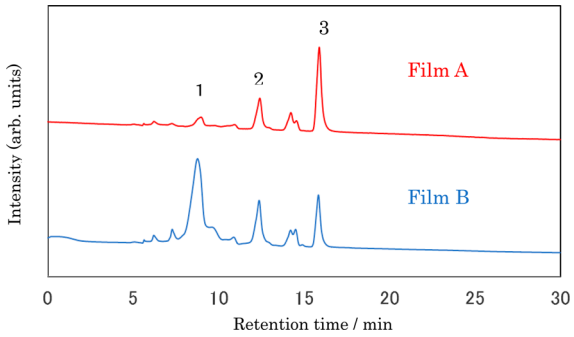

Figure 4. HPLC chromatograms of the KOH solutions which dissolved eosin Y from films A and B.

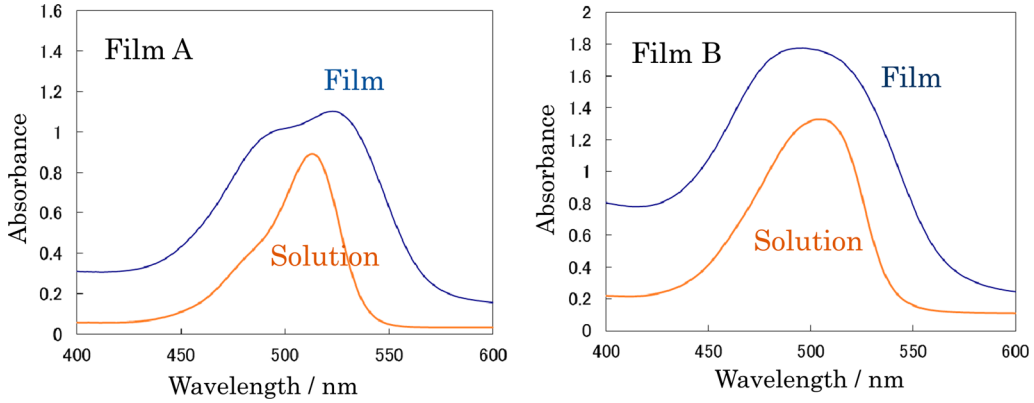

Figure 3. Absorption spectra of films A and B prepared after the treatments with the 0.060 and 1.2 mmol dm^{-3} $PdCl_2$ solutions, respectively, and the KOH aqueous solutions which dissolved the eosin Y from films A and B.

DOI: 10.1021/acsami.5b02570
ACS Appl. Mater. Interfaces 2015, 7, 11592−11598

On the basis of a comparison between the relative strength of peak 1 and peak 2 and that of peak 3, that of peak 1 and peak 2 for film B was greater than that for film A. The intensity of peak 1 was stronger than that of peak 2 for film B, indicating that peak 1 was related to the difference in the absorption spectra of the films. Table S1 (Supporting Information) shows the identified molecular species from the ESI-MS measurements of these three peaks. It was suggested that peak 1, peak 2, and peak 3 were the eosin Y-dianion didebrominated and monodebrominated species and the original eosin Y-dianion, respectively. It was clear that the amount of the eosin Y debrominated species in film B was greater than that in film A. Furthermore, on the basis of a comparison between the spectra of film B and the KOH solution prepared from film B, it is suggested that not only the eosin Y debromination species but also the eosin Y dimer existed in the film because the absorbance at 490 nm in the film was greater than that of the KOH solution.

To investigate the eosin Y debromination, the eosin Y-adsorbing ZnO films were prepared under various conditions, i.e., with and without DMAB and 1.2 mmol dm^{-3} $PdCl_2$ treatment, by electrodeposition. Figure S1 (Supporting Information) shows the absorption spectra of the samples. It was confirmed that the DMAB addition and $PdCl_2$ treatment are necessary to obtain the film having a peak at 490 nm.

The FT-IR spectra of the film samples and eosin Y sodium salt indicated that the eosin Y dianion coordinated to the ZnO through an ester-like linkage and carboxylate linkage as shown in Figure S2 (Supporting Information).

As the amount of Pd on the substrate surface increased, the reduction by DMAB in the solution should be significantly promoted. During this process, eosin Y was not only adsorbed on the ZnO surface but also simultaneously reduced and debrominated. As a result, the eosin Y species adsorbed on the ZnO surface were the monomer, dimer, and debromination species. It was confirmed that the Pd particles on the surface catalyzed the reduction and sequential debromination of eosin Y by DMAB.

3.2. Characterization of ZnO films. Figure 5 shows the SEM images of the surface of the samples prepared in the deposition bath with and without eosin Y after the treatment with the different concentrations of $PdCl_2$ solutions. The film samples prepared with no $PdCl_2$ treatment or eosin Y, no $PdCl_2$ treatment and eosin Y, 0.060 mmol dm^{-3} $PdCl_2$ solution and eosin Y, and 1.2 mmol dm^{-3} $PdCl_2$ solution and eosin Y were labeled Pd0, Pd0-EY, Pd0.06-EY, and Pd1.2-EY, respectively. The deposition time was changed so that the film thickness was approximately the same. On the basis of a comparison between these films, their morphologies were quite different. The ZnO crystals in Pd0 grew linearly and vertically on the substrate surface. The (0002) plane in the wurtzite ZnO was observed in the SEM image. The flake-shaped crystals stood vertically on the substrate surface and were very densely packed in Pd0-EY. In Pd0.06-EY and Pd1.2-EY, there were large pores among the spherical ZnO particles. The particles size of Pd0.06-EY was larger than that of Pd1.2-EY. Furthermore, the particles with diameters of around 10−50 nm were aggregated and formed the secondary particles in Pd0.06-EY and Pd1.2-EY. The secondary particles seemed to form a hexagonal structure. The particle size estimated from the SEM images were ca. 50, 130, 250, and 150 nm for Pd0, Pd0-EY, Pd0.06-EY, and Pd1.2-EY, respectively.

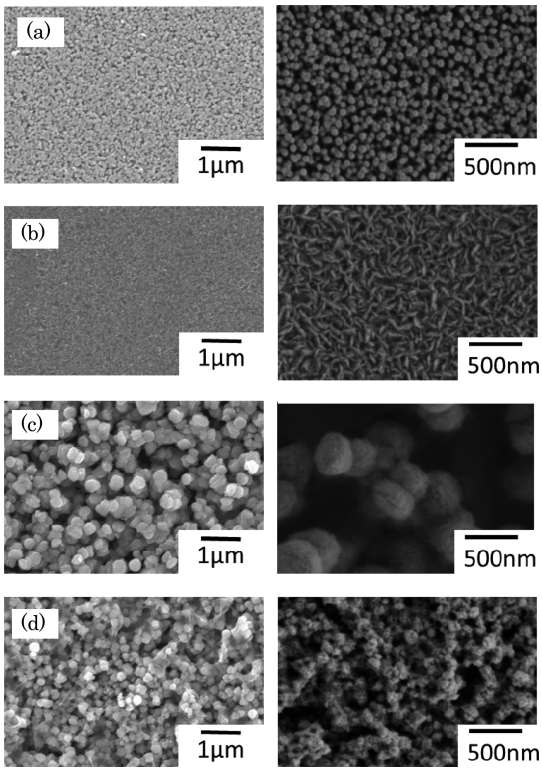

Figure 5. SEM images of the surface of (a) Pd0, (b) Pd0-EY, (c) Pd0.06-EY, and (d) Pd1.2-EY.

Figure 6 shows the XRD patterns of the films and ZnO powder. Their film thickness was ca. 1.3−1.5 μm. The XRD patterns indicated that the relative intensities of the (0002) and (1011) peaks were stronger than those of the other peaks in Pd0 and Pd0-EY, respectively. These results corresponded to the SEM images. The ZnO crystals preferred to grow in the *c*-axis direction in Pd0 because the (0002) plane has the highest surface energy and polarity in the wurtzite ZnO.[23] These results supported the belief that the eosin Y molecules were preferentially adsorbed on the (0002) plane of ZnO.[24] The XRD patterns of Pd0.06-EY and Pd1.2-EY were similar to that of the ZnO powder. Pd1.2-EY had a higher crystallinity because the peak intensity of Pd1.2-EY was higher than that of Pd0.06-EY.

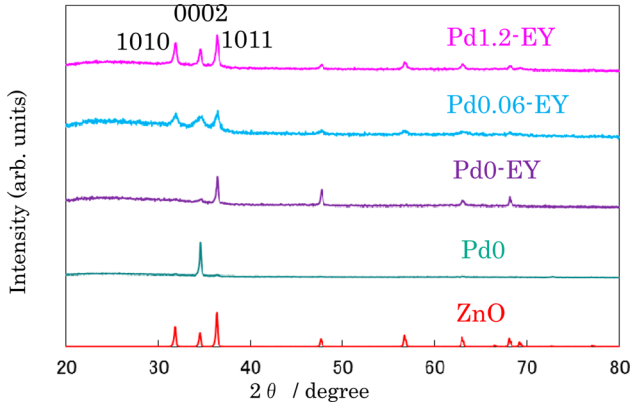

Figure 6. XRD patterns of ZnO powder, Pd0, Pd0-EY, Pd0.06-EY, and Pd1.2-EY.

DOI: 10.1021/acsami.5b02570
ACS Appl. Mater. Interfaces 2015, 7, 11592−11598

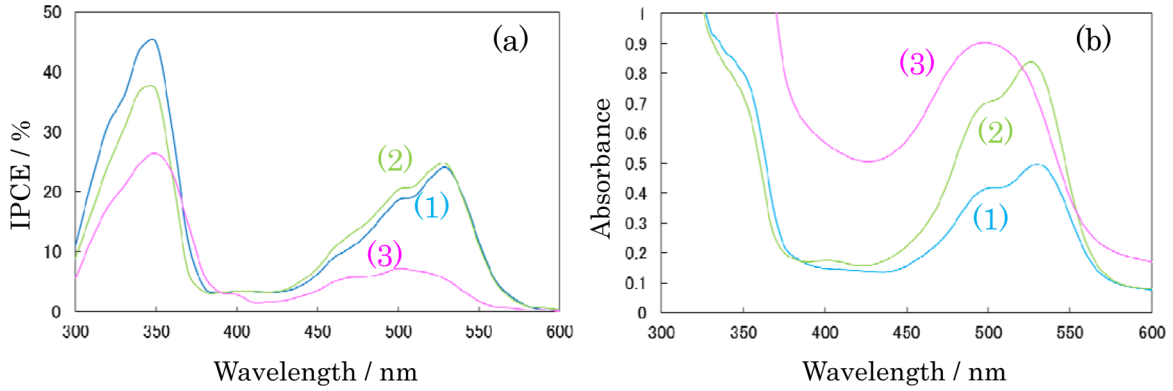

Figure 7. (a) IPCE and (b) absorption spectra of (1) Pd0-EY, (2) Pd0.06-EY, and (3) Pd1.2-EY.

As already described, for the electroless deposition process, eq 1 depended on the amount of Pd on the substrate surface. Without Pd on the substrate, the ZnO particles prefer to grow in the *c*-axis direction perpendicular to the (0002) plane as observed in Pd0, whereas in the presence of eosin Y in the solution, the (0002) peak intensity decreased because the eosin Y molecules were preferentially adsorbed on the (0002) plane of ZnO.[17] As a result, the ZnO preferred to grow in the direction of the *a*-axis or *b*-axis, and formed flake-shaped particles vertical to the substrate as observed in Pd0-EY. Matsushima et al.[25] reported that the orientation of ZnO prepared by liquid-phase deposition changed from (0002) to (1011) to (1010) by adding carboxylic acid to the solution. Pd0-EY exhibited the same tendency because eosin Y has a carboxyl group in its molecular structure.

As the amount of Pd increased, the formation rate of ZnO nuclei was faster. Therefore, a significant number of ZnO nuclei were immediately formed and the crystal growth produced a smaller size. The orientation was suppressed and a random orientation was observed in Pd0.06-EY and Pd1.2-EY. The secondary particles in Pd0.06-EY were larger than those of Pd1.2-EY. This indicated that the smaller ZnO particles in Pd0.06-EY were more aggregated than those of Pd1.2-EY. Therefore, Pd0.06-EY had a lower crystallinity than Pd1.2-EY based on the XRD patterns.

During the initial stage of the ZnO deposition, the ZnO particles growing to ca.10−50 nm were aggregated and formed larger secondary particles as the deposition proceeded. In the ZnO growth process, eosin Y was adsorbed on the ZnO. In the absence of the Pd on the substrate surface, the ZnO nucleation rate was slow. The eosin Y adsorbed on the surface of the ZnO crystal eventually formed the monomer or dimer. The monomer was preferably adsorbed under this condition. In the presence of the Pd on the substrate surface, the ZnO nucleation successively proceeded and a large amount of ZnO particles were formed. Eosin Y was also reduced and simultaneously debrominated by DMAB. As a result, not only the monomer and dimer but also the debrominated species of eosin Y were adsorbed on the ZnO and incorporated in the ZnO secondary particles.

As the dye-adsorbing film prepared without the Pd was washed with ethanol, the ethanol was red-colored and exhibited an absorption peak at 520 nm. However, in the film prepared with Pd having a peak at 490 nm, the color did not become lighter. In this film, it is suggested that eosin Y is hard to be desorbed due to the interaction with the ZnO aggregated particles.

3.3. Photoelectric Conversion Properties of the Eosin Y-Adsorbing ZnO Films. Figure 7 shows the photocurrent action spectra and absorption spectra of the samples. The photocurrent only slightly depended on the existence of the Pd particles because the amount of Pd was much lower than that of ZnO based on the EDS measurement (Pd < 0.1%). The Pd particles did not function as a catalyst of the surface reaction during the electrochemical measurements because they were incorporated in the ZnO particles. The maximum incident photon-to-current conversion efficiency (IPCE) values in the range from 400 to 600 nm were 0.24, 0.25, and 0.07 for Pd0-EY, Pd0.06-EY, and Pd1.2-EY, respectively. The maximum absorbed photon-to-current quantum efficiency (APCE) values in the UV (350 nm) and visible (510−530 nm) ranges, which originated from the excitation of the ZnO and the eosin Y, respectively, were estimated to discuss the electron injection process from the dye. Table 1 shows the APCE values in the

Table 1. Photocurrent Internal Quantum Efficiency Values in the UV and Visible Ranges and Their Ratios for the Eosin Y-Adsorbing ZnO Electrodes

electrode	UV range (A)	visible range (B)	ratio (B/A)
Pd0-EY	0.53 (350 nm)	0.35 (530 nm)	0.66
Pd0.06-EY	0.46 (350 nm)	0.29 (530 nm)	0.63
Pd1.2-EY	0.26 (350 nm)	0.08 (510 nm)	0.31

UV and visible ranges and their ratios, which depended on the efficiency of the electron injection from the dye. The IPCE and APCE values of Pd1.2-EY from 400 to 600 nm were quite low. The eosin Y species were mainly the monomer in Pd0-EY and Pd0.06-EY and the dimer and debrominated species in Pd1.2-EY. The halogenated derivatives of such molecules led to fluorescence quenching and facilitated the energy transfer from the molecules to ZnO.[26] Therefore, it is suggested that the debromination of eosin Y decreased the sensitization effect.[27] Although the absorbance of Pd0.06-EY from 400 to 600 nm was 2 times larger than that of Pd0-EY, the IPCE values were nearly equal. The film resistance can increase because the eosin Y molecules were incorporated between the ZnO secondary particles in Pd0.06-EY. The absorption from 300 to 400 nm depended on the ZnO band structure. Although the ZnO in Pd1.2-EY had a higher crystallinity than that of Pd0.06-EY based on the X-ray diffraction patterns, the IPCE and APCE values in the UV range for Pd1.2-EY were lower. The APCE values at 350 nm for the ZnO samples, from which eosin Y was extracted with a KOH aqueous solution, were also lower in the

DOI: 10.1021/acsami.5b02570
ACS Appl. Mater. Interfaces 2015, 7, 11592−11598

order of Pd1.2-EY, Pd0.06-EY, and Pd0-EY, depending on the resistance of the ZnO films. The visible absorbance of Pd1.2-EY was greater than that of Pd0.06-EY depending on the dye content. However, the IPCE and APCE values in the UV and visible ranges for Pd1.2-EY were lower than those for Pd-0.06EY due to the high resistance of the ZnO film. The ratio of the APCE value in the visible range to that in the UV range for Pd1.2-EY was significantly lower than those for the other samples. On the basis of the APCE values, it was suggested that the electron injection efficiency from the monomer was more efficient than that from the other species.

The photocurrent value for Pd0-EY decreased due to dye desorption or degradation during the light irradiation and was 70% of the initial value after the 1-h irradiation. The stability of the adsorbed dye was similar to that on the titania film.[28] The improvement of the dye stability is a subject in the next study.

Figure 8 shows the $J-V$ curves of the samples and their energy conversion efficiencies (η). The short circuit photo-

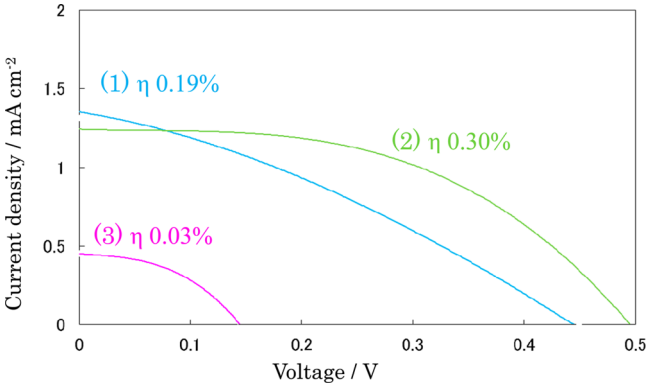

Figure 8. $J-V$ curves of (1) Pd0-EY, (2) Pd0.06-EY, and (3) Pd1.2-EY.

current densities corresponded to the photocurrent spectral values in the range from 450 to 520 nm. The value for Pd1.2-EY was much lower than that for Pd-0.06EY. The energy conversion efficiencies for the present samples were much lower than those for the eosin Y-adsorbing ZnO films prepared by electrodeposition, dye desorption, and readsorption (2.7%)[21] due to the thinness of the ZnO films (ca. 1.3−1.5 μm) and low dye amount. The internal energy conversion efficiencies, i.e., the energy conversion efficiencies relative to the total energy of the absorbed photons, were 3.3%, 2.8%, and 0.1% for Pd0-EY, Pd0.06-EY, and Pd1.2-EY, respectively. It is expected that the energy conversion efficiencies will be improved by an increase in the film thickness and optimization of the dye adsorption.

4. CONCLUSION

Thin films consisting of ZnO or eosin Y-adsorbing ZnO particles were prepared on FTO substrates by electroless deposition from aqueous solutions containing $Zn(NO_3)_2$ and DMAB in the absence or presence of eosin Y at 328 K. The surface structure of the ZnO particles was characterized and their spectroscopic and photoelectric conversion properties were evaluated by photoelectrochemical measurements. We investigated the influences of the eosin Y species and the Pd particles as a catalyst, which were deposited on the substrate surface by the $PdCl_2$ treatment, on the particle formation process and photoelectric properties. Without Pd on the substrate, the ZnO particles prefer to grow in the c-axis direction perpendicular to the (0002) plane in the absence of eosin Y in the solution, whereas in the presence of eosin Y, the (0002) peak intensity decreased because the eosin Y molecules were preferentially adsorbed on the (0002) plane of ZnO. As a result, the ZnO preferred to grow in the direction of the a-axis or b-axis, and formed flake-shaped particles vertical to the substrate surface. On the basis of the amount of the Pd particles, the eosin Y species adsorbed on the ZnO were considerably changed and affected the growth of the ZnO particles. As the Pd particles were adsorbed on the substrate, not only the eosin Y monomer but also the dimer and debrominated species were rapidly adsorbed on the spherical ZnO particles, which were aggregated and formed secondary particles. However, in the absence of the Pd particles, the monomer was adsorbed on the flake-shaped ZnO particles, which grew vertically on the substrate surface and had a high crystallinity. The photoelectric conversion efficiency was higher for the ZnO electrodes containing a higher amount of the monomer during light irradiation.

■ ASSOCIATED CONTENT

Supporting Information

The Supporting Information is available free of charge on the ACS Publications website at DOI: 10.1021/acsami.5b02570.

■ AUTHOR INFORMATION

Corresponding Author

*Tel.: +81-26-269-5536. Fax: +81-26-269-5531. E-mail: nishiki@shinshu-u.ac.jp.

Notes

The authors declare no competing financial interest.

■ REFERENCES

(1) Matsuoka, M. Synthetic Design of Infrared Absorbing Dyes. *Infrared Absorbing Dyes* **1990**, 7−17.
(2) Sanz-Menez, N.; Monnier, V.; Colombier, I.; Baldeck, P. L.; Irie, M.; Ibanez, A. Photochromic Fluorescent Diarylethene Nanocrystals Grown in Sol−Gel Thin Films. *Dyes Pigm.* **2011**, *89*, 241−245.
(3) Matsuda, K.; Irie, M. Diarylethene as a Photoswitching Unit. *J. Photochem. Photobiol., C* **2004**, *5*, 169−182.
(4) Shirinian, V. Z.; Besugliy, S. O.; Metelitsa, A. V.; Krayushkin, M. M.; Nikalin, D. M.; Minkin, V. I. Novel Photochromic Spirocyclic Compounds of Thienopyrroline Series: 1: Spiropyrans. *J. Photochem. Photobiol., A* **2007**, *189*, 161−166.
(5) Galvin, J. M.; Schuster, G. B. Preparation and Characterization of Mixed Thin Films Containing Spiropyrans and Long Chain Alkyl Silanes: Towards a Command Surface for Liquid Crystal Realignment. *Supramol. Sci.* **1998**, *5*, 89−100.
(6) Zhang, B.; Zhao, W.; Cao, Y.; Wang, X.; Zhang, Z.; Jiang, X.; Xu, S. Photoluminescence and Electroluminescence of Squarylium Cyanine Dyes. *Synth. Met.* **1997**, *91*, 237−241.
(7) De, S.; Das, S.; Girigoswami, A. Environmental Effects on the Aggregation of Some Xanthene Dyes Used in Lasers. *Spectrochim. Acta, Part A* **2005**, *61*, 1821−1833.
(8) Kim, J. Y. High Performance of the Organic−Inorganic Powder Electroluminescence Device with High Color-rendering Capability Using the Multilayer. *Opt. Commun.* **2014**, *321*, 86−89.
(9) Li, Y.; Guo, M.; Peng, S.; Lu, G.; Li, S. Formation of Multilayer-Eosin Y-Sensitized TiO2 via Fe^{3+} Coupling for Efficient Visible-Light Photocatalytic Hydrogen Evolution. *Int. J. Hydrogen Energy* **2009**, *34*, 5629−5636.
(10) Regan, B.; Gratzel, M. A Low-Cost, High-Efficiency Solar Cell Based on Dye-Sensitized Colloidal TiO_2 Films. *Nature* **1991**, *353*, 737−740.

DOI: 10.1021/acsami.5b02570
ACS Appl. Mater. Interfaces 2015, 7, 11592−11598

(11) Izaki, M.; Omi, T. Transparent Zinc Oxide Films Prepared by Electrochemical Reaction. *Appl. Phys. Lett.* **1996**, *68*, 2439−2440.
(12) Peulen, S.; Lincot, D. Mechanistic Study of Cathodic Electrodeposition of Zinc Oxide and Zinc Hydroxychloride Films from Oxygenated Aqueous Zinc Chloride Solutions. *J. Electrochem. Soc.* **1998**, *145*, 864−874.
(13) Izaki, M.; Omi, T. Transparent Zinc Oxide Films Chemically Prepared from Aqueous Solution. *J. Electrochem. Soc.* **1997**, *144*, L3−L5.
(14) Yoshida, T.; Terada, K.; Schlettwein, D.; Oekermann, T.; Sugiura, T.; Minoura, H. Electrochemical Self-Assembly of Nanoporous ZnO/Eosin Y Thin Films and Their Sensitized Photoelectrochemical Performance. *Adv. Mater.* **2000**, *16*, 1214−1217.
(15) Yoshida, T.; Minoura, H. Electrochemical Self-Assembly of Dye-Modified Zinc Oxide Thin Films. *Adv. Mater.* **2000**, *16*, 1219−1222.
(16) Yoshida, T.; Tochimoto, M.; Schlettwein, D.; Wohrle, D.; Sugiura, T.; Minoura, H. Self-Assembly of Zinc Oxide Thin Films Modified with Tetrasulfonated Metallophthalocyanines by One-Step Electrodeposition. *Chem. Mater.* **1999**, *11*, 2657−2667.
(17) Nagaya, S.; Nishikiori, H. Preparation of Dye-Adsorbing ZnO Thin Films by Electroless Deposition and Their Photoelectrochemical Properties. *ACS Appl. Mater. Interfaces* **2013**, *5*, 8841−8844.
(18) Izaki, M.; Katayama, J. Characterization of Boron-Incorporated Zinc Oxide Film Chemically Prepared from an Aqueous Solution. *J. Electrochem. Soc.* **2000**, *147*, 210−213.
(19) Cameron, P. J.; Peter, L. M. Characterization of Titanium Dioxide Blocking Layers in Dye-Sensitized Nanocrystalline Solar Cells. *J. Phys. Chem. B* **2003**, *107*, 14394−14400.
(20) Lu, W.; Schmidt, H. Synthesis of Tin Oxide Hydrate ($SnO_2 \cdot xH_2O$) Gel and Its Effects on the Hydrothermal Preparation of $BaSnO_3$ Powders. *Adv. Powder Technol.* **2008**, *19*, 1−12.
(21) Yoshida, T.; Zhang, J.; Komatsu, D.; Sawatani, S.; Minoura, H.; Pauporte, T.; Lincot, D.; Oekermann, T.; Schlettwein, D.; Tada, H.; Wohrle, D.; Funabiki, K.; Matsui, M.; Miura, H.; Yanagi, H. Electrodeposition of Inorganic/Organic Hybrid Thin Films. *Adv. Funct. Mater.* **2009**, *19*, 17−43.
(22) Rohatgi, K. K.; Mukhopadhyay, A. K. Isolation of Unique Dimer Spectra of Dyes from the Composite Spectra of Aggregated Solutions. *Photochem. Photobiol.* **1971**, *14*, 551−559.
(23) Kong, X. Y.; Wang, Z. L. Polar-Surface Dominated ZnO Nanobelts and the Electrostatic Energy Induced Nanohelixes, Nanosprings, and Nanospirals. *Appl. Phys. Lett.* **2004**, *84*, 975−977.
(24) Wagata, H.; Ohashi, N.; Taniguchi, T.; Katsumata, K.; Okada, K.; Matsushita, N. Control of the Microstructure and Crystalline Orientation of ZnO Films on a Seed-free Glass Substrate by Using a Spin-Spray Method. *Cryst. Growth Des.* **2010**, *10*, 4968−4975.
(25) Matsushita, N.; Wagata, H.; Ohashi, N.; Okada, K. Method for Producing Conductive Zinc Oxide Film. U.S. Patent 20140008109A1, Jan 5, 2012.
(26) Lee, S. H.; Kim, J. H.; Park, C. B. Coupling Photocatalysis and Redox Biocatalysis Toward Biocatalyzed Artificial Photosynthesis. *Chem.-Eur. J.* **2013**, *19*, 4392−4406.
(27) Sayama, K.; Sugino, M.; Sugihara, H.; Abe, Y.; Arakawa, H. Photosensitization of Porous TiO_2 Semiconductor Electrode with Xanthene Dyes. *Chem. Lett.* **1998**, *27*, 753−754.
(28) Nishikiori, H.; Teshima, K.; Fujii, T. Photoinduced Electron Transfer in Rhodamine B-Containing Amorphous Titania Gels. *Res. Chem. Intermed.*. DOI 10.1007/s11164-013-1490-8.

DOI: 10.1021/acsami.5b02570
ACS Appl. Mater. Interfaces 2015, 7, 11592−11598